Enhancement in the spectral irradiance of photoconducting terahertz emitters by chirped-pulse mixing

Aniruddha S. Weling and Tony F. Heinz

Departments of Physics and Electrical Engineering, Columbia University, New York, New York 10027

Received March 25, 1999

We describe the use of mixing linearly chirped optical pulses in biased photoconductors to generate tunable narrow-band terahertz (THz) radiation with enhanced spectral brightness. The increase in conversion efficiency from optical to THz radiation at a given THz frequency arises from the improved saturation characteristics of the photoconductor for chirped-pulse mixing compared with the usual case of excitation by an ultrafast optical pulse. In the weak saturation limit, the enhancement in the saturation fluence scales with the ratio of the duration of the chirped optical pulse to the photocurrent relaxation time in the emitter and is essentially independent of the beat frequency generated by the chirped-pulse mixing technique. This dependence allows for substantial enhancements in the saturation fluence and, hence, in the THz spectral brightness. We demonstrate enhanced saturation fluences experimentally for dipole emitters fabricated on radiation-damaged Si on sapphire. © 1999 Optical Society of America [S0740-3224(99)00608-6]

OCIS codes: 320.7160, 320.5540, 260.5150, 230.0250.

1. INTRODUCTION

Recently several ultrafast optoelectronic techniques were developed to generate subpicosecond pulses of coherent terahertz (THz) radiation propagating in free space.[1–4] The most commonly used technique for generating such bursts of intense far-infrared radiation relies on the optical excitation of radiative current transients in biased photo-conductors.[1,4] Coupled with synchronously gated, phase-coherent detectors based on either photoconductive[1,2] or electro-optic sampling,[5] these THz emitters have provided powerful tools for time-domain THz spectroscopy of a variety of systems,[6] THz imaging,[7] and impulse ranging of objects.[8] The THz radiation emitted from photoconductors has also been used as a sensitive probe of the subpicosecond dynamics of photoexcited carriers in these devices,[9] which ultimately defines the limits of their performance. Further, large-area photoconducting THz emitters permit certain investigations that involve high-intensity THz radiation, such as the study of atoms and molecules in strong transient electric fields.[10]

Large-aperture photoconducting emitters have been shown to be efficient optoelectronic sources of highly directional beams of freely propagating THz radiation.[11] Such broadband THz emitters can be scaled to high THz powers without loss of speed or of THz bandwidth, which is limited only by the photocurrent rise time.[12] However, the radiated fields from these emitters saturate with increasing optical fluence and constrain the THz output. Such saturation effects are seen in photoconductive emitters at laser fluences as low as 10–100 μJ/cm^2,[12,13] which are well below fluences that can be achieved by common ultrafast laser sources as well as below the optical damage thresholds of photoconductive media. Thus possible methods for circumventing these saturation effects are desirable so that the full capabilities of current femtosecond laser systems can be used for generating intense far-infrared radiation. The development of high-brightness coherent THz sources should facilitate new linear and nonlinear spectroscopic measurements in the far-infrared region.[9,14]

In this paper we discuss the improved saturation characteristics and enhanced spectral brightness of these emitters obtainable for optical excitation that is appropriately shaped in time.[15] One such scheme for shaping femtosecond optical excitation is offered by the chirped-pulse beating scheme that we demonstrated recently for generating narrow-band THz radiation.[16] Applying this scheme can reduce saturation effects in photoconducting THz emitters by a significant degree, thereby enhancing the THz spectral brightness at any frequency within the emission bandwidth. In Section 3 below, we present calculations of this enhancement in the THz spectral brightness of large-aperture photoconducting emitters within the framework of a model of saturation effects previously developed for the case of short optical excitation pulses. In addition to providing this analytical and numerical treatment, in Section 4 we report experimental results that demonstrate an enhancement in the saturation fluence of photoconducting dipole emitters. Similar enhancements in narrow-band THz generation were reported recently by Liu *et al.*, who used femtosecond pulse-shaping techniques to achieve quasi-sinusoidal optical modulation.[17]

2. CHIRPED-PULSE MIXING

Although the broadband THz generation schemes that utilize femtosecond laser pulses are powerful and well suited for many applications, certain investigations in the far infrared may benefit from either tunable narrow-band

0740-3224/99/091455-13$15.00

THz generation or detection capabilities. To this end, we introduced a method of incorporating spectral selectivity in both the generation and the coherent detection of freely propagating THz radiation.[16,18] This technique involves the optical heterodyning of two linearly chirped optical pulses with a variable time delay τ between them to produce a quasi-sinusoidal intensity modulation at tunable THz frequencies. A square-law photomixer such as a $\chi^{(2)}$ medium or a photoconductor can then convert this quasi-sinusoidal optical modulation into pulses of narrow-band THz radiation. One can tune the center frequency of the THz radiation generated simply by varying the delay τ between the two chirped optical pulses.[16,18] It is our purpose in this paper to demonstrate that the saturation characteristics for photoconductive emitters under excitation obtained by mixing such stretched optical pulses are significantly improved relative to their saturation behavior for short-pulse excitation.

First we examine the expected behavior for the generation of broadband and narrow-band THz radiation by the conventional and chirped-pulse mixing schemes, respectively, in the absence of saturation. In this regime the generation process can be described quite generally in terms of the production of a nonlinear polarization from the second-order nonlinear response of the medium. This description obviously applies to nonresonant nonlinear media. It applies equally well to biased photoconductors, although the magnitude and the THz frequency dependence of the response will clearly differ in the two cases. We work here in the frequency domain and denote the Fourier transform of the pump (laser) field as $\mathbf{E}_{\mathrm{in}}(\omega)$. It follows that the Fourier transform of the induced nonlinear polarization at any THz frequency Ω within the base band of the optical pulse may be written as

$$\mathbf{P}_{\mathrm{NL}}(\Omega) = \chi^{(2)}(\Omega){:}\int_{-\infty}^{\infty} \mathrm{d}\omega \mathbf{E}_{\mathrm{in}}(\omega + \Omega)\mathbf{E}_{\mathrm{in}}^{*}(\omega). \quad (1)$$

In Eq. (1) we assume only that the nonlinear response tensor $\chi^{(2)}(\Omega)$ involved in the optical rectification process has negligible dispersion at the optical frequencies of the pump beam.

We may apply this analysis either to a transform-limited broadband optical pulse or to the case of chirped-pulse mixing. For the latter case, the presence of a linear chirp is equivalent in the frequency domain to multiplication by a phase factor $\exp[\, j(\omega - \omega_0)^2/2\mu]$, where ω_0 denotes the center frequency of the laser spectrum and μ represents the rate of frequency sweep. A replica of this pulse separated from it by a time delay τ can be described by an additional phase factor $\exp[\, j(\omega - \omega_0)\tau]$. The relevant term in the difference-frequency mixing of a pair of such linearly chirped optical pulses, each with energy equal to that in the unchirped pulse, is then

$$\begin{aligned}\mathbf{P}_{\mathrm{NL}}(\Omega) = \chi^{(2)}(\Omega){:}\int_{-\infty}^{\infty} \mathrm{d}\omega \mathbf{E}_{\mathrm{in}}(\omega + \Omega) \\ \times \exp[\, j(\omega - \omega_0 + \Omega)^2/2\mu]\mathbf{E}_{\mathrm{in}}^{*}(\omega) \\ \times \exp[-j(\omega - \omega_0)^2/2\mu - j\tau(\omega - \omega_0)]. \quad (2)\end{aligned}$$

On comparing Eqs. (1) and (2), we see immediately that they are identical when we choose a delay time of $\tau = \Omega/\mu$ (to within an unimportant overall phase factor), corresponding to a beat frequency Ω for the chirped pulses. Because the radiated THz field $\mathbf{E}(\Omega)$ is determined by $\mathbf{P}^{\mathrm{NL}}(\Omega)$, this result implies that the THz output at any frequency Ω within the THz power spectrum is equivalent for the broadband THz emission produced by a single unchirped pulse and the narrow-band THz output from the chirped-pulse mixing process for the appropriate delay time. Therefore the process of mixing two time-delayed chirped optical pulses in a $\chi^{(2)}$ material is equivalent to linear filtering of the broadband THz output for a single transform-limited optical pulse with an energy equal to that of either of the chirped pulses.

For the purposes of our discussion it is convenient to introduce the spectral irradiance of the THz emission, which is given by

$$S(\Omega) = R(c\varepsilon_0/2)|\mathbf{E}(\Omega)|^2. \quad (3)$$

Here $\mathbf{E}(\Omega)$ is the Fourier transform of the THz field produced by a single excitation pulse and R is the repetition rate of these pulses. $S(\Omega)$ corresponds to the average THz power radiated per unit area of the emitter (radiant exitance) per unit bandwidth.[19] It is clear from the above discussion that, for low-excitation fluences, the THz spectral irradiance $S(\Omega)$ of the narrow-band THz emission produced by chirped-pulse mixing is equal to that for the broadband THz radiation generated by an unstretched pulse of the same energy as each of the chirped pulses. This equivalence is not, however, maintained at optical fluences where the THz output starts to be limited by saturation effects.

3. SATURATION OF THE TERAHERTZ FIELD IN PHOTOCONDUCTORS

Before embarking on a detailed discussion of the saturation processes in photoconductors, we would like to provide a physical explanation for the origin of saturation and the amelioration of these effects attainable by use of optical pulse-shaping techniques such as chirped-pulse mixing. In a biased photoconductor, THz radiation arises from the transport of optically injected carriers that are driven by a static (bias) field. In many photoconductors, rapid relaxation of the photogenerated carriers occurs either by nonradiative recombination at traps or by sweep-out of carriers from the active region. The transient photocurrent induced by a femtosecond laser pulse (and, consequently, the radiated THz field) varies linearly with the optical pulse energy until the photogenerated carrier density becomes large enough to screen the bias field. In the case of a planar large-aperture photoconductor, saturation of the THz output occurs when the strength of the radiated THz field at the surface of the emitter matches that of the applied dc bias, thus eliminating the driving force for the transient current. Although the details of the physical mechanism of saturation of the peak THz field in photoconducting devices depend on the structure of the emitter,[12,20,21] the critical factor that determines the onset of saturation is generally the maximum density of carriers injected by the exciting laser pulse.

The saturation fluence of a THz emitter can be defined as the excitation fluence at which the THz pulse energy starts to deviate appreciably from its ideal quadratic variation with the pump pulse energy. In our analysis we consider the case of photoconductive emitters excited by a quasi-sinusoidally modulated optical pump pulse whose duration is much longer than the photocurrent relaxation process in the emitter. This excitation corresponds to that obtained by the chirped-pulse mixing scheme. The increase in the saturation fluence obtained in this case compared with that for a pump pulse much shorter than the photocurrent decay time (broadband THz) can be understood in terms of the peak carrier density injected in the two cases. The number density of carriers per unit area generated in a photoconductor illuminated by a time-varying optical irradiance $I_{\mathrm{in}}(t)$ can be expressed as

$$N(t) = \frac{\beta}{\hbar\omega}\int_{-\infty}^{t} dt' I_{\mathrm{in}}(t')\exp\left[-\frac{(t-t')}{\tau_d}\right], \qquad (4)$$

where the pump photon energy $\hbar\omega$ is greater than the bandgap of the photoconductor, β is the fraction of the laser energy absorbed, and τ_d denotes the photocurrent relaxation time. The maximum carrier density generated is then proportional to the optical energy absorbed by the photoconductor over a period that corresponds to τ_d. Thus saturation of the THz field from such an emitter is expected whenever a certain optical fluence is deposited over a time interval of the order of the photocurrent relaxation time.

Let us consider the chirped-pulse mixing scheme with the duration of the stretched optical pulse being much greater than the photocurrent relaxation time in the THz emitter. In this case, the time-varying excitation $I_{\mathrm{in}}(t)$ is spread over many such decay time intervals, and, consequently, a higher total fluence can be utilized without entering the saturation regime. For the chosen THz beat frequency, the radiation from all these time intervals within the excitation pulse adds together coherently, allowing for the generation of THz radiation of increased spectral irradiance at that frequency. The enhancement in the optical fluence at which saturation occurs should therefore scale with the ratio of the duration of the stretched pulse to the photocurrent relaxation time. This effect is illustrated schematically in Fig. 1, which shows a comparison of the THz power spectrum [i.e., $S(\Omega)$] for narrow-band and broadband excitation in both the low-fluence and saturation limits. In the following sections we show that enhancements as large as 10^3 are predicted in the THz spectral irradiance $S(\Omega)$ for stretched optical pulses of ~100-ps duration and photoconductors with subpicosecond carrier relaxation times.

A. Model for Saturation in Photoconductive Terahertz Emitters

To examine the nature of saturation effects for chirped-pulse beating in a more quantitative fashion, we have applied the model developed by Darrow *et al.*[12] and Taylor and co-workers[13,21–23] to describe the saturation behavior of the THz radiation from large-aperture photoconductive emitters. We chose the large-aperture emitters for detailed analysis because they offer the most favorable structure for high-intensity THz radiation. Furthermore, saturation effects in these structures have been investigated and may be described by an attractive and relatively simple theory. In such planar structures, saturation arises primarily from screening of the dc bias field by the radiated THz electric field that is present at the surface of the emitter.[12,13] Further, in contrast to the case of emitters for which the transient photocurrent flows normal to the surface (such as p–i–n diodes and the surface depletion regions of unbiased semiconductors[20]), screening from space-charge effects is weak.[21,23] Although in the analysis presented below we assume that the emitter is a large-area photoconductor, similar saturation effects are also important for other planar structures such as photoconducting dipole emitters used in our experiments.

The radiated THz field at a point close to the uniformly illuminated surface of a planar THz emitter excited by normally incident laser radiation is given by[12]

$$\mathbf{E}(t) = -\left(\frac{\eta_0}{1+n}\right)\mathbf{J}(t) = -\eta'\mathbf{J}(t). \qquad (5)$$

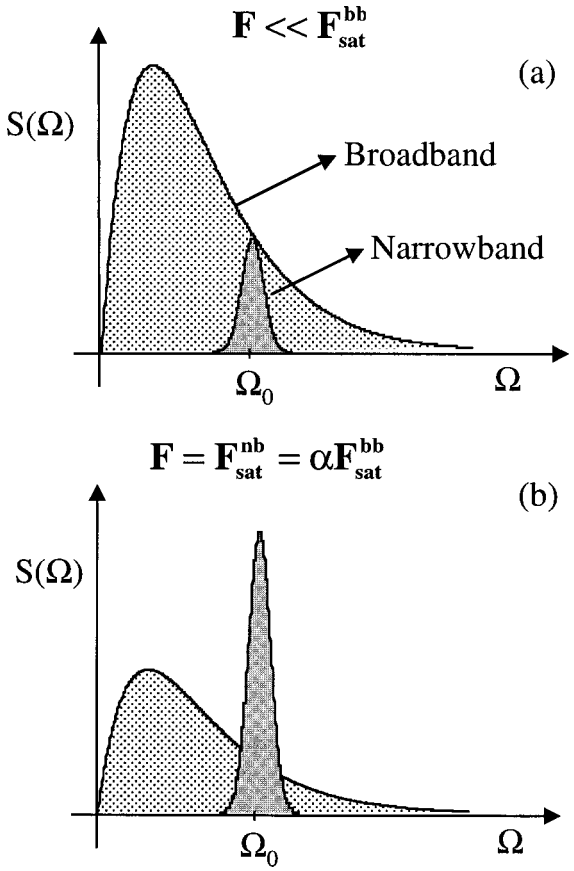

Fig. 1. Schematic illustration of the enhancement in THz spectral irradiance from an enhanced saturation fluence for the case of narrow-band excitation. The THz output is illustrated for (a) the low-fluence case in which chirped-pulse mixing is equivalent to spectral filtering of the broadband THz output and (b) the high-fluence case in which broadband output is saturated while narrow-band saturation is just incipient. The saturation fluences for broadband ($F_{\mathrm{bb}}^{\mathrm{sat}}$) and narrow-band ($F_{\mathrm{nb}}^{\mathrm{sat}}$) excitation are discussed in Subsection 3.B of the text.

In Eq. (5), η_0 is the impedance of free space (377 Ω), n is the index of refraction of the photoconducting material at THz wavelengths, and we write $\eta' = \eta_0/(1 + n)$ for convenience. $\mathbf{J}(t)$ denotes the surface photocurrent density, which is related to the bias field $\mathbf{E}_b$ by[12]

$$\mathbf{J}(t) = \frac{\sigma(t)\mathbf{E}_b}{\sigma(t)\eta' + 1}. \tag{6}$$

These relations are derived by use of boundary conditions at the surface of the THz emitter and include all the relevant Fresnel factors. The central assumption here is that the photoconductor is large and illuminated uniformly over a length scale much greater than the THz wavelength.[12,13] The time-dependent surface conductivity $\sigma(t)$ in Eq. (6) is related to the transient mobility $\mu(t)$ and the photogenerated carrier density $N(t)$ by

$$\sigma(t) = e\int_{-\infty}^{t} dt'\mu(t - t')N(t'), \tag{7}$$

where e is the electron charge. If we introduce a Drude model for the transient mobility of the photoconductor [i.e., an exponential with a rise time τ_r (Ref. 6)], we may rewrite Eq. (7) as

$$\sigma(t) = K\int_{-\infty}^{t} dt' \frac{\exp[-(t - t')/\tau_r]}{\tau_r} \int_{-\infty}^{t'} dt'' \times \exp[-(t' - t'')/\tau_d] I(t''). \tag{8}$$

Here the constant $K \equiv e\mu_{\mathrm{dc}}/\hbar\omega$, with μ_{dc} denoting the low-frequency mobility, and we have made use of Eq. (4) to relate the carrier density to the absorbed laser irradiance $I(t)$ [i.e., $I(t) = \beta I_{\mathrm{in}}(t)$]. This simplified picture of the transient photoconductivity has proved effective in modeling of broadband THz emission for both large-aperture[12,13] and dipole[6] emitters.

B. Analysis of Saturation for Narrow-Band Excitation

In our analysis of narrow-band THz emission we shall be concerned with quantities that vary in time in a quasi-sinusoidal fashion with an envelope that changes slowly compared with the frequency of the oscillation. We treat these quantities within the slowly varying amplitude approximation. We may then write any real time-dependent function $F(t)$ that oscillates at frequency Ω as

$$F(t) = F^0(t) + \mathrm{Re}[F^{\Omega}(t)\exp(j\Omega t)], \tag{9}$$

where $F^{\Omega}(t)$ denotes the envelope function at frequency Ω and $F^0(t)$ denotes the dc component. This representation is used below for all the narrow-band quantities, such as optical irradiance $I(t)$, photocurrent density $J(t)$, and radiated THz field $E(t)$.

To proceed with the analysis of saturation effects, we now introduce the form for the narrow-band laser excitation of the emitter. For a substantially stretched laser pulse in the chirped-pulse mixing scheme, we may write the laser irradiance of the two combined beams as

$$I(t) = I^0(t) + \mathrm{Re}[I^{\Omega}(t)\exp(j\Omega t)]. \tag{10}$$

As was discussed above, we can readily vary the modulation frequency Ω, which must lie within the base band of the laser pulse, by changing the time delay between the two interfering pulses.[18] Although we may consider Eq. (10) as a generalized form for narrow-band laser excitation of the emitter, we may also write explicit expressions for the envelope functions for chirped-pulse mixing. In this case the total optical irradiance for ideal narrow-band excitation is given by[18]

$$I(t) = I_0(t) + I_0(t + \tau) + 2[I_0(t)I_0(t + \tau)]^{1/2}\cos\Omega t. \tag{11}$$

Here τ is the time delay between the two chirped excitation pulses, $\Omega = \mu\tau$ is the beat frequency, and an unimportant phase factor has been omitted from the last term. From this expression we readily obtain the envelope functions of Eq. (10) as

$$I^0(t) = I_0(t) + I_0(t + \tau),$$

$$I^{\Omega}(t) = 2[I_0(t)I_0(t + \tau)]^{1/2}. \tag{12}$$

We use these equations below to evaluate the enhancements in the narrow-band THz output obtained for the specific case of chirped-pulse mixing. For now, we continue our analysis with a generalized narrow-band excitation $I(t)$ of the form defined by Eq. (10). For such an excitation profile we can obtain the following expression for the transient surface conductivity $\sigma(t)$ from Eq. (8) above:

$$\sigma(t) \approx KI^0(t)\tau_d + K\tau_d\,\mathrm{Re}\left[\frac{I^{\Omega}(t)\exp(j\Omega t)}{(1 + j\Omega\tau_d)(1 + j\Omega\tau_r)}\right] = \sigma^0(t) + \mathrm{Re}[\sigma^{\Omega}(t)\exp(j\Omega t)]. \tag{13}$$

Here we assume that the temporal width of $I(t)$ is much greater than the time constants τ_r and τ_d. We see that the surface conductivity $\sigma(t)$ has a zero-frequency component $\sigma^0(t) = KI^0(t)\tau_d$ and a component $\sigma^{\Omega}(t) = K\tau_d^{\Omega}I^{\Omega}(t)$ at the driving frequency Ω, with a complex time constant τ_d^{Ω} given by

$$\tau_d^{\Omega} \equiv \frac{\tau_d}{(1 + j\Omega\tau_r)(1 + j\Omega\tau_d)}. \tag{14}$$

To examine the saturation properties of the THz emitter, we consider the variation of the THz output with pump laser irradiance, i.e., the dependence of spectral irradiance $S(\Omega)$ on absorbed optical irradiance $I(t)$. For the purpose of discussion, we introduce a saturation parameter θ that characterizes the degree of saturation through

$$\theta \equiv \frac{S_i(\Omega) - S(\Omega)}{S_i(\Omega)}, \tag{15}$$

where the subscript i denotes the ideal behavior that would be expected in the absence of saturation effects. The parameter θ varies from a value 0 in the absence of

saturation (low pump fluence) to a value approaching 1 for strong saturation (high pump fluence).

We can evaluate saturation parameter θ conveniently in the present framework by taking spectral irradiance $S(\Omega)$ for narrow-band excitation to be proportional to the time-averaged irradiance S of the narrow-band THz emission. Within the slowly varying amplitude approximation we may write

$$S = R(c\varepsilon_0/2)\int_{-\infty}^{\infty}|E^{\Omega}(t)|^2 \mathrm{d}t, \tag{16}$$

where R is the repetition rate of the THz pulses. This approach, which neglects the fluence-dependent changes in the line shape of the narrow-band THz emission, leads to

$$\theta \equiv \frac{S_i(\Omega) - S(\Omega)}{S_i(\Omega)} \approx \left.\frac{S_i - S}{S_i}\right|_{\Omega} = \frac{\int_{-\infty}^{\infty}\mathrm{d}t[|E_i^{\Omega}(t)|^2 - |E^{\Omega}(t)|^2]}{\int_{-\infty}^{\infty}\mathrm{d}t|E_i^{\Omega}(t)|^2}. \tag{17}$$

To complete our analytic treatment, we assume that saturation remains relatively weak; i.e., we examine the range of pump fluence where the deviation from ideal behavior is small ($\theta \ll 1$). In this limit, Eq. (6) for the photocurrent can be linearized to yield the effective screening field at any THz frequency Ω. To this end, we express the surface photocurrent density as

$$\mathbf{J}(t) = \mathbf{J}_i(t) + \Delta\mathbf{J}(t), \tag{18}$$

where $\mathbf{J}_i(t)$ is the ideal surface current density $\mathbf{J}_i(t) = \sigma(t)\mathbf{E}_b$ that would be present in the absence of saturation. The deviation $\Delta\mathbf{J}(t)$ caused by the presence of near-field screening of the bias field can be approximated from Eq. (6) as

$$\Delta\mathbf{J}(t) \approx -\mathbf{E}_b\eta'[\sigma(t)]^2 = -\mathbf{E}_b\eta'\{\sigma^0(t) + \mathrm{Re}[\sigma^{\Omega}(t)\exp(j\Omega t)]\}^2. \tag{19}$$

If we expand this expression, we find that

$$\Delta\mathbf{J}^{\Omega}(t) \approx -2\eta'\sigma^{\Omega}(t)\sigma^0(t)\mathbf{E}_b = -2\eta' K^2\tau_d\tau_d^{\Omega}I^0(t)I^{\Omega}(t)\mathbf{E}_b \tag{20}$$

for the component of $\Delta\mathbf{J}(t)$ at driving frequency Ω. Analogously, photocurrent density $\mathbf{J}_i(t)$ in the ideal case has the following component at driving frequency Ω:

$$\mathbf{J}_i^{\Omega}(t) = \sigma^{\Omega}(t)\mathbf{E}_b = KI^{\Omega}(t)\tau_d^{\Omega}\mathbf{E}_b. \tag{21}$$

Expression (20) above implies that the relative deviation from ideality in the narrow-band photocurrent density at any frequency Ω ($\Delta\mathbf{J}^{\Omega}/\mathbf{J}_i^{\Omega}$) is proportional to the dc conductivity $\sigma^0(t) = KI^0(t)\tau_d$ and is independent of $\sigma^{\Omega}(t)$. Hence, to first order, the degree of saturation in the THz output is determined by time constant τ_d and slowly varying envelope $I^0(t)$ of the excitation pulse and is independent of Ω.

Inasmuch as THz field $\mathbf{E}(t)$ is directly proportional to photocurrent density $\mathbf{J}(t)$ [Eq. (5)], expression (17) for the narrow-band saturation parameter can be written as

$$\theta = \frac{\int_{-\infty}^{\infty}\mathrm{d}t[|J_i^{\Omega}(t)|^2 - |J^{\Omega}(t)|^2]}{\int_{-\infty}^{\infty}\mathrm{d}t|J_i^{\Omega}(t)|^2} \approx 2\frac{\int_{-\infty}^{\infty}\mathrm{d}t\,\mathrm{Re}\{[J_i^{\Omega}(t)]^*\Delta J^{\Omega}(t)\}}{\int_{-\infty}^{\infty}\mathrm{d}t|J_i^{\Omega}(t)|^2}. \tag{22}$$

The latter relation applies in the weak saturation limit, where we may neglect the term that is proportional to $|\Delta J^{\Omega}(t)|^2$ in the expansion of the integrand of the numerator. Using expressions (20) and (21) to obtain the components of the photocurrent $\mathbf{J}_i(t)$ and $\Delta\mathbf{J}(t)$ at THz excitation frequency Ω, we have

$$\theta = 4K\tau_d\eta'\frac{\int_{-\infty}^{\infty}I^0(t)|I^{\Omega}(t)|^2\mathrm{d}t}{\int_{-\infty}^{\infty}|I^{\Omega}(t)|^2\mathrm{d}t}. \tag{23}$$

We shall now rewrite this expression after identifying some of the relevant quantities. We first introduce a parameter $F_{\mathrm{sat}}^{\mathrm{bb}}$ to describe the characteristic absorbed fluence at which saturation is reached for broadband THz emission:

$$F_{\mathrm{sat}}^{\mathrm{bb}} = \frac{(\sqrt{2}-1)}{K\eta'} = (\sqrt{2}-1)\left(\frac{1+n}{\eta_0}\right)\frac{\hbar\omega}{e\mu_{\mathrm{dc}}}. \tag{24}$$

As can be seen from Eqs. (5), (6), and (8), this is the absorbed fluence at which the peak amplitude of THz field $E(t)$ is equal to $1/\sqrt{2}$ of its value in the absence of saturation effects. This description of $F_{\mathrm{sat}}^{\mathrm{bb}}$ assumes that the laser pulse duration is much shorter than the rise time τ_r, which is, in turn, much shorter than τ_d. The value of $F_{\mathrm{sat}}^{\mathrm{bb}}$ for an arbitrary excitation pulse will include a dimensionless factor that is a function of τ_r and τ_d. It should be noted that the present definition of saturation fluence differs by a numerical factor from the definition used previously.[12,13] This definition corresponds to the fluence at which the THz field amplitude reaches half of its maximum value. Consequently, it is a factor of $(\sqrt{2}-1)^{-1}$ higher than the value adopted in our analysis, which corresponds approximately to $\theta = 0.5$ in saturation of the THz irradiance. Although such a frequency-independent definition of the saturation fluence is distinct from that used in our analysis of saturation of the narrow-band THz emission, it nevertheless serves to estimate the excitation fluence above which the spectral irradiance at any frequency within the power spectrum of the broadband THz

output does not change appreciably. We further note that the absorbed fluence in the narrow-band excitation is

$$F^{\mathrm{nb}} = \int_{-\infty}^{\infty} \mathrm{d}t I(t) = \int_{-\infty}^{\infty} \mathrm{d}t I^0(t). \tag{25}$$

In terms of these quantities, we may rewrite Eq. (23) for the saturation parameter as

$$\theta = \frac{1}{2} \frac{F^{\mathrm{nb}}}{F_{\mathrm{sat}}^{\mathrm{bb}}} \left(\frac{\tau_d}{T_{\mathrm{eff}}} \right). \tag{26}$$

In Eq. (26) we have defined an effective pulse duration T_{eff} of the narrow-band optical excitation as

$$T_{\mathrm{eff}} = \frac{(\sqrt{2}+1) \int_{-\infty}^{\infty} |I^{\Omega}(t)|^2 \mathrm{d}t \int_{-\infty}^{\infty} I^0(t) \mathrm{d}t}{8 \int_{-\infty}^{\infty} I^0(t) |I^{\Omega}(t)|^2 \mathrm{d}t}. \tag{27}$$

For the case of narrow-band excitation derived from chirped-pulse mixing, we can express T_{eff} as a function of the irradiance envelope $I_0(t)$ of the stretched pulse and of the delay time τ:

$$T_{\mathrm{eff}} = \frac{(\sqrt{2}+1) \left[\int_{-\infty}^{\infty} I_0(t) I_0(t+\tau) \mathrm{d}t \right] \int_{-\infty}^{\infty} I_0(t) \mathrm{d}t}{4 \int_{-\infty}^{\infty} [I_0^2(t) I_0(t+\tau) + I_0^2(t+\tau) I_0(t)] \mathrm{d}t}. \tag{28}$$

From Eq. (26), for the saturation behavior, we may further identify a narrow-band fluence $F^{\mathrm{nb}} = F_{\mathrm{sat}}^{\mathrm{nb}}$ at which the relative deviation from ideality is 50% ($\theta = 0.5$) as

$$F_{\mathrm{sat}}^{\mathrm{nb}} = F_{\mathrm{sat}}^{\mathrm{bb}} (T_{\mathrm{eff}}/\tau_d). \tag{29}$$

The enhancement in the saturation fluence for the narrow-band excitation compared with broadband excitation is thus given by the ratio of the effective stretched pulse duration to the carrier relaxation time. Hence we may write

$$\alpha \equiv F_{\mathrm{sat}}^{\mathrm{nb}}/F_{\mathrm{sat}}^{\mathrm{bb}} = T_{\mathrm{eff}}/\tau_d, \tag{30}$$

where, for convenience, we have introduced a dimensionless parameter α, defined as the ratio of the saturation fluences for the two methods of excitation. This represents the quantitative formulation of the heuristic discussion of Section 2. The enhancement in the saturation fluence is thus inversely proportional to decay time τ_d and exhibits only a weak dependence on beat frequency Ω (through T_{eff}).

To illustrate this enhancement more quantitatively, we consider the case of narrow-band excitation with a modulated Gaussian pulse of the form

$$\begin{aligned} I(t) &= I_0 \exp(-t^2/T^2)(1+\cos \Omega t) \\ &= I_0 \exp(-t^2/T^2) + \mathrm{Re}[I_0 \exp(-t^2/T^2) \exp(j\Omega t)]. \end{aligned} \tag{31}$$

Such quasi-sinusoidal excitation is obtained by mixing of two linearly chirped broadband pulses that have Gaussian envelopes at a small delay $\tau \ll T$. For such pulses the dc and oscillatory envelope functions are simply $I^0(t) = I^{\Omega}(t) = I_0 \exp(-t^2/T^2)$, and we obtain from Eq. (27) an effective pulse width of

$$T_{\mathrm{eff}} = \left(\frac{(\sqrt{2}+1)}{8} \sqrt{\frac{3\pi}{2}} \right) T \approx 0.655T. \tag{32}$$

For a Gaussian envelope with a duration of 100 ps (FWHM), which corresponds to $T \cong 60$ ps, Eq. (30) yields an enhancement of the order of $\alpha = (39.3/\tau_d)$ in the saturation fluence in a photoconductor with a photocurrent relaxation time of τ_d ps.

We now consider the enhancement in the THz spectral irradiance $S(\Omega)$ that ensues from the predicted enhancement in the saturation fluence of the emitter under narrow-band excitation. For this purpose we compare the spectral irradiance at any frequency Ω for narrow-band and broadband THz generation at their respective saturation fluences. Using the definition of the broadband saturation fluence $F_{\mathrm{sat}}^{\mathrm{bb}}$, we may express the broadband THz output at saturation as

$$S_{\mathrm{sat}}^{\mathrm{bb}} \equiv S^{\mathrm{bb}}|_{F=F_{\mathrm{sat}}^{\mathrm{bb}}} = (1/2) S_i^{\mathrm{bb}}|_{F=F_{\mathrm{sat}}^{\mathrm{bb}}}. \tag{33}$$

The frequency-independent value that we have assumed for the broadband THz saturation fluence is suitable for the purposes of predicting general trends. Similarly, we may express the narrow-band THz output at saturation by

$$S_{\mathrm{sat}}^{\mathrm{nb}} \equiv S^{\mathrm{nb}}|_{F=F_{\mathrm{sat}}^{\mathrm{nb}}} = (1/2) S_i^{\mathrm{nb}}|_{F=F_{\mathrm{sat}}^{\mathrm{nb}}}. \tag{34}$$

By combining the two relations above and making use of the scaling for THz emission in the unsaturated regime, we obtain an estimate of the increase in the spectral irradiance at saturation for narrow-band emission compared with broadband emission:

$$S_{\mathrm{sat}}^{\mathrm{nb}}/S_{\mathrm{sat}}^{\mathrm{bb}} = (F_{\mathrm{sat}}^{\mathrm{nb}}/F_{\mathrm{sat}}^{\mathrm{bb}})^2 = \alpha^2 = (T_{\mathrm{eff}}/\tau_d)^2. \tag{35}$$

Another quantity of interest in this comparison of the two excitation schemes is the optical-to-THz conversion efficiency η at saturation. The enhancement obtained in this conversion efficiency for the narrow-band case may be written as

$$\frac{\eta_{\mathrm{sat}}^{\mathrm{nb}}}{\eta_{\mathrm{sat}}^{\mathrm{bb}}} \equiv \frac{S_{\mathrm{sat}}^{\mathrm{nb}}/F_{\mathrm{sat}}^{\mathrm{nb}}}{S_{\mathrm{sat}}^{\mathrm{bb}}/F_{\mathrm{sat}}^{\mathrm{bb}}} = \alpha = \frac{T_{\mathrm{eff}}}{\tau_d}. \tag{36}$$

C. Numerical Calculations

In this section we present some results of numerical calculations of the THz radiation from a large-aperture photoconducting emitter as a function of the pump pulse energy, using the same model as defined above by Eqs. (5), (6), and (8). These calculations are intended to complement the approximate analytic treatment by investigations of the regime of highly saturated THz emission and to provide evaluation of the expressions for enhancements in the saturation fluence for representative material parameters.

In our calculations of transient conductivity $\sigma(t)$, we assume a carrier scattering time of $\tau_r = 0.27$ ps (Ref. 6) and a decay time of $\tau_d = 0.6$ ps,[23] parameters that are appropriate for radiation-damaged Si on sapphire (RDSOS), the photoconductor used in our experiments. For the dc mobility μ_{dc} of RDSOS we take the previously measured value of 30 $cm^2/V\,s$.[1,12] The laser excitation of the sample for the broadband case is assumed to be a Gaussian pulse with a duration of 100 fs FWHM. The narrow-band excitation corresponds to mixing two linearly chirped Gaussian pulses, each with an energy and bandwidth equivalent to those of the 100-fs pulse.

Figure 2 displays the calculated THz spectral irradiance $S(\Omega)$ for narrow-band excitation at three beat frequencies as a function of the absorbed optical fluence for excitation by a pair of chirped pulses with a duration of 100 ps FWHM. The figure also shows the variation of the corresponding quantity for excitation with a broadband pulse of the same energy as each of the chirped pulses. In the low-fluence limit, the spectral brightness of the narrow-band THz emission is equal to that of the broadband THz case [Eqs. (1) and (2)]. However, as shown in Fig. 2, the THz emission characteristics for the chirped-pulse mixing case retain the ideal quadratic fluence dependence over a considerable range of pump fluences for which the broadband THz emission is already saturated. It should be noted that, at fluences well above the point of deviation from ideal behavior shown in Fig. 2, the nonlinear relation between the photocurrent and the laser irradiance [Eq. (6)] gives rise to a complicated redistribution of the THz power within the emission spectrum. This phenomenon is also evident in the narrow-band case, for which the THz power goes into harmonics of the beat frequency. Thus the characteristics in the regime of strong saturation differ somewhat, depending on the THz emission frequency.

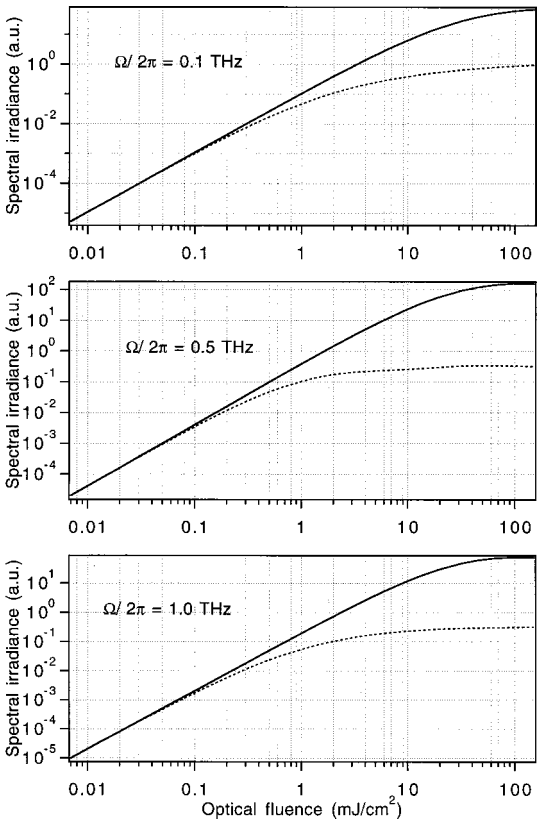

Fig. 2. Results of numerical calculations of the variation of THz spectral irradiance $S(\Omega)$ with absorbed optical fluence for three frequencies Ω within the emission spectrum of a large-aperture RDSOS photoconducting emitter for broadband (dotted curves) and narrow-band (solid curves) excitation. The broadband excitation pulses are Gaussian with $T_{bb} = 100$ fs (FWHM), and the narrow-band excitation pulses are obtained by mixing of linearly chirped Gaussian pulses with $T_{nb} = 100$ ps (FWHM). For these calculations, based on the saturation model described in the text, the following parameters were assumed: $\tau_r = 0.27$ ps, $\tau_d = 0.6$ ps, $\mu_{dc} = 30\ cm^2/V\,s$.

Figure 3 illustrates the dependence of narrow-band saturation fluence F_{sat}^{nb} on various important parameters. As discussed above, we define F_{sat}^{nb} as the absorbed fluence at which a 50% decrease in THz spectral brightness $S(\Omega)$ from ideal behavior is reached ($\theta = 0.5$). Figure 3(a) shows the variation of F_{sat}^{nb} with photocurrent relaxation time τ_d at the three THz beat frequencies used for the data plotted in Fig. 2. From the numerically calculated values, we see that the dependence of F_{sat}^{nb} on decay time τ_d agrees nicely with the $1/\tau_d$ relationship predicted in Eq. (29). For a photocurrent decay time of 0.6 ps (τ_d for RDSOS), we also verified the absence of any significant dependence of F_{sat}^{nb} on rise time τ_r for values of $\tau_r < \tau_d = 0.6$ ps. We repeated the above calculations with a different envelope function, chosen as $I_0(t) = I_0\,\mathrm{sech}^2(t/T)$, for the chirped pulses and observed similar trends in the narrow-band saturation fluence.

The variation of F_{sat}^{nb} with THz emission frequency Ω is depicted in Fig. 3(b) for a photocurrent relaxation time $\tau_d = 0.6$ ps. The dependence of F_{sat}^{nb} on Ω is seen to be quite weak. This behavior arises from the fact that the screening field that affects the THz output at any frequency Ω is largely independent of Ω, as is apparent in the weak saturation analysis from expression (20). The numerically calculated value of F_{sat}^{nb} is comparable with the estimate of 22.1 mJ/cm^2 obtained from the analytical treatment of Eqs. (30) and (32) for 100-ps-long Gaussian pulses. Because the perturbation treatment is only approximate at a saturation of $\theta = 0.5$, precise agreement is not expected. Figure 3(c) illustrates the dependence of the narrow-band saturation fluence on the duration (FWHM) of the chirped optical pulses at the three beat frequencies examined in Fig. 3(a). As predicted by Eq. (29), F_{sat}^{nb} scales linearly with stretched pulse width T. Only when pulse widths much shorter than 100 ps ($\leqslant$5 ps) are considered does this behavior begin to break down. This is a consequence of the failure of the slowly varying amplitude approximation, which was central to our analysis.

Figure 4 shows the calculated enhancement in spectral irradiance $S(\Omega)$ of the narrow-band THz output compared with that of the broadband THz emission at the narrow-band saturation fluence F_{sat}^{nb}. This enhancement is plotted as a function of photocurrent relaxation time τ_d at the same beat frequencies as in Fig. 3(a). Unlike in Subsection 3.B, where we examined the narrow-band and broadband spectral irradiance at their respective saturation fluences, here we consider the output of the two excitation schemes at a fluence of F_{sat}^{nb}. If we wish to com-

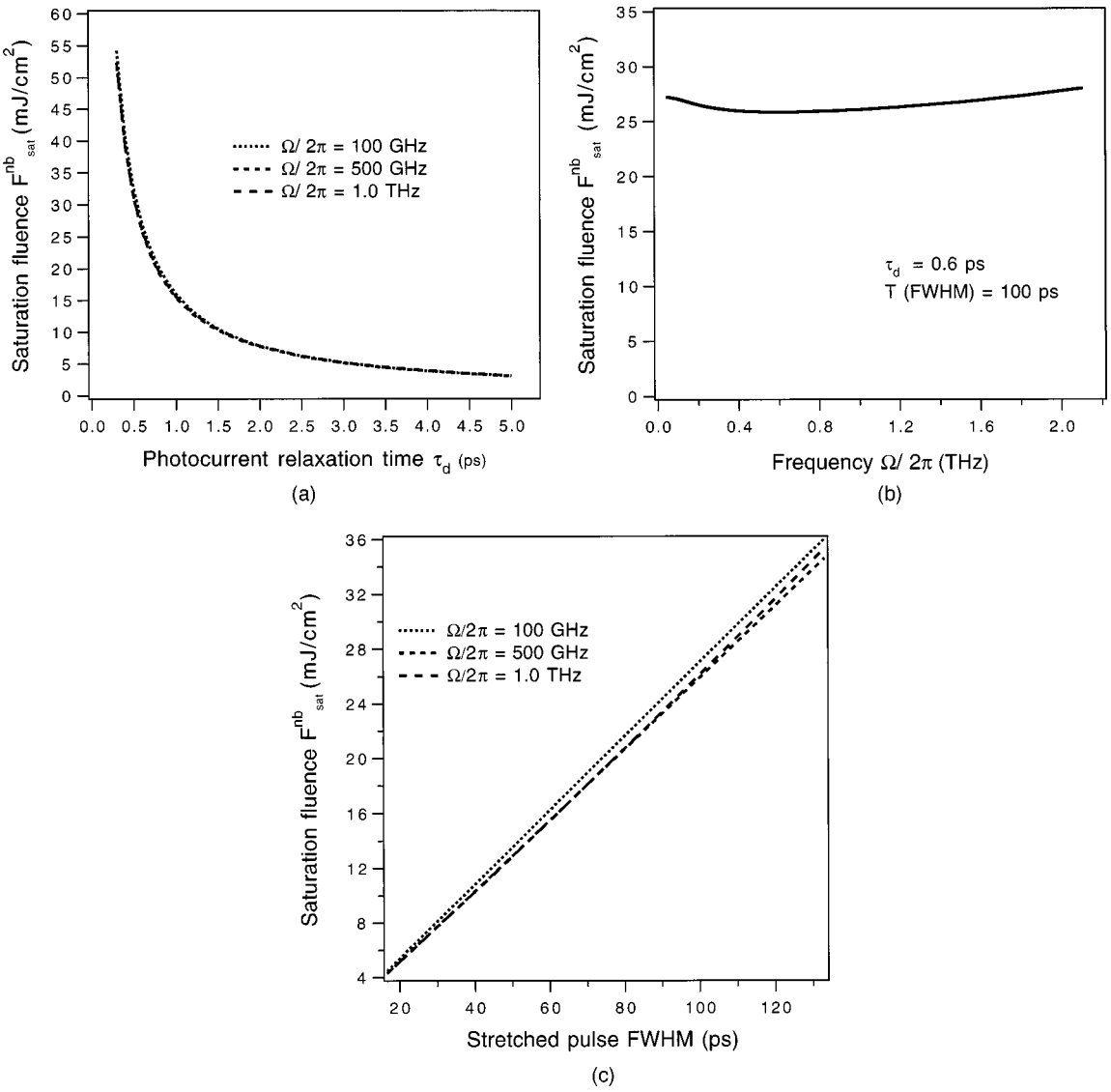

Fig. 3. Results of numerical calculations for narrow-band saturation fluence F^{nb}_{sat} (fluence at 50% deviation from ideal behavior): (a) Dependence of F^{nb}_{sat} on photocurrent relaxation time τ_d for mixing of 100-ps-long (FWHM) chirped Gaussian pulses at beat frequencies Ω of 100 and 500 GHz and 1.0 THz. (b) Dependence of F^{nb}_{sat} on THz beat frequency Ω for chirped Gaussian pulses with values of τ_d and T shown. (c) Dependence of F^{nb}_{sat} on the duration (FWHM) of the chirped Gaussian pulses for $\tau_d = 0.6$ ps at the three THz beat frequencies given in (a).

pare these numerical results with those produced by the analytic treatment, we need to estimate the value of broadband spectral irradiance S^{bb} at a fluence of F^{nb}_{sat}. We can accomplish this by assuming that the spectral irradiance has already reached its maximum saturated value. Using the functional form suggested by Eq. (6), we may estimate

$$S^{bb}|_{F=F^{sat}_{nb}} \approx S^{bb}_{max} = S^{bb}_{sat}\left(\frac{\sqrt{2}}{\sqrt{2}-1}\right)^2 \cong 11.66 S^{bb}_{sat}. \quad (37)$$

Combining this result with Eq. (35), we deduce the following expression for effective enhancement in the spectral irradiance at F^{nb}_{sat}:

$$\left.\frac{S^{nb}}{S^{bb}}\right|_{F=F^{nb}_{sat}} = \frac{S^{nb}_{sat}}{S^{bb}_{sat}}\left(\frac{S^{bb}_{sat}}{S^{bb}|_{F=F^{nb}_{sat}}}\right) \cong \frac{\alpha^2}{11.66}. \quad (38)$$

Taking $\alpha = T_{eff}/\tau_d$ then yields an explicit prediction for the enhancement in spectral irradiance at a fluence that corresponds to narrow-band saturation. The corresponding relation is plotted in Fig. 4. (There is, in principle, a dependence of T_{eff} on THz frequency Ω; it is slight over the range of frequencies considered and has been neglected for clarity.)

A comparison of the analytic approximation for the enhancement in the spectral irradiance with the numerical simulations reveals similar trends. The numerical results show a magnitude of the enhancement that is generally comparable with the analytic result and roughly re-

produce the predicted scaling with $(1/\tau_d)^2$. On the other hand, the degree of agreement between the analytic result and the numerical simulation depends rather strongly on the THz emission frequency Ω that is under consideration. This situation may be attributed primarily to the existence of a frequency dependence in the saturation process, a factor neglected in the analytic treatment. More specifically, at fluences of the order of $F_{\mathrm{sat}}^{\mathrm{nb}}$, the broadband THz output is strongly in the saturation regime and undergoes significant redistribution of $S(\Omega)$ within the THz power spectrum. This behavior reflects the fact that saturation in photocurrent $J(t)$ limits the peak value of THz field $E(t)$, which cannot exceed bias field E_b, without restricting the total energy in the THz pulse. Hence the actual saturation characteristics of $S(\Omega)$ may have an appreciable dependence on THz frequency Ω, as may be observed by inspection of the numerically calculated THz output characteristics of Fig. 2. This frequency dependence and the breakdown of the analytic approximation are especially pronounced for short photocurrent relaxation times τ_d. This is not unexpected: low values of τ_d correspond to the regime of large enhancements in the saturation fluence and, consequently, to broadband emission in the regime of strong saturation, where changes in the shape of the THz emission spectrum should be most significant.

D. Discussion

An issue that merits further discussion concerns the influence of the choice of the photoconductive medium on the expected narrow-band and broadband emission properties. Both the analytic treatment and the numerical calculations indicate that narrow-band saturation fluence $F_{\mathrm{sat}}^{\mathrm{nb}}$ scales with the parameter T_{eff}/τ_d. Therefore, to obtain the highest possible enhancement α in the saturation fluence it is desirable to use the longest optical excitation pulse and the shortest relaxation time τ_d attainable experimentally. Whereas the former criterion requires an optimal experimental geometry (which imposes minimal cubic and higher-order phase distortion on the chirped laser pulses), the latter requirement entails the choice of an appropriate photoconducting material. For example, in the case of RDSOS, a photocurrent decay time as short as $\tau_d = 0.6$ ps is expected. For chirped Gaussian pulses of 100-ps duration, the analytic theory then predicts an enhancement in the saturation fluence of $\alpha = 65.5$ and a corresponding enhancement in the spectral irradiance $S(\Omega)$ of the order of $\alpha^2/11.7 \approx 370$. The numerical calculations presented in Figs. 2 and 4 predict an enhancement of ~240 in $S(\Omega)$ at a pump fluence that corresponds to the numerically calculated $F_{\mathrm{sat}}^{\mathrm{nb}} = 26\ \mathrm{mJ/cm^2}$ at a frequency of 500 GHz (close to the peak of the broadband THz power spectrum). Of course, if the material has a substantially longer photocurrent relaxation time, the predicted enhancement will decrease accordingly.

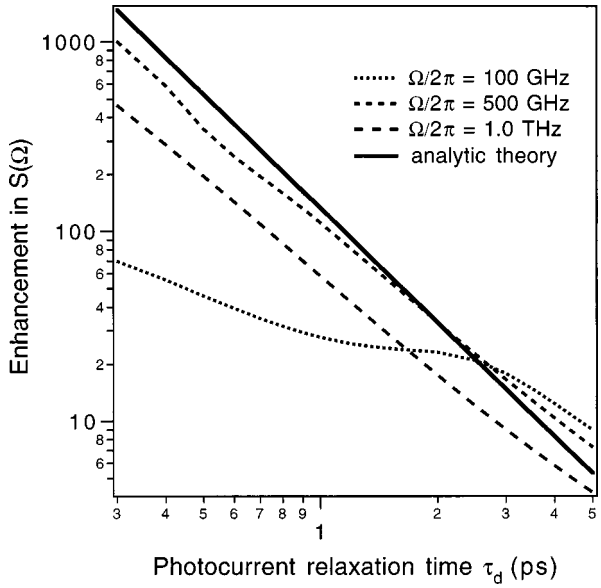

Fig. 4. Calculated enhancement in spectral irradiance $S(\Omega)$ at the three THz beat frequencies of Fig. 3(a) of the narrow-band THz output obtained by mixing of 100-ps-long chirped Gaussian pulses compared with the linearly filtered broadband THz output obtained from a single 100-fs Gaussian pulse. This enhancement is determined for a pump fluence yielding a 50% deviation from ideal behavior in the narrow-band case ($F_{\mathrm{sat}}^{\mathrm{nb}}$) and is plotted as a function of photocurrent relaxation time τ_d. The prediction of the simple analytical theory presented in Subsection 3.B is also shown.

Within the context of the present theory and discussion, increasing the ratio of the chirped-pulse duration to the photocurrent relaxation time may increase the spectral brightness arbitrarily. To achieve this limit, however, the saturation fluence increases without bound, and effects not considered in our analysis may begin to be significant. More specifically, to realize fully the predicted enhancements in the THz spectral irradiance we must be able to apply pump fluences up to a value of $F_{\mathrm{sat}}^{\mathrm{nb}}$. In the case of photoconductive emitters based on RDSOS, our analysis indicates that, for stretched pulses of 100-ps duration, optical fluences in excess of 10 $\mathrm{mJ/cm^2}$ are required for optimal conversion efficiency. Fluences of this magnitude are sufficiently high that various processes, such as sample heating and pump-induced changes in the dielectric response of the medium, that were neglected in our analysis may become significant. The nature and importance of these additional constraints will clearly depend on the characteristics of the sample and the duration of the stretched optical pulses. As shown in Eq. (29), we may estimate the optimal pump fluence by $F_{\mathrm{sat}}^{\mathrm{nb}} = (T_{\mathrm{eff}}/\tau_d)F_{\mathrm{sat}}^{\mathrm{bb}}$. The characteristics of the sample enter through the photocurrent relaxation time τ_d, as well as the value of the broadband saturation fluence $F_{\mathrm{sat}}^{\mathrm{bb}} = [(1 + n)/\eta_0]\hbar\omega/e\mu_{\mathrm{dc}}$ [Eq. (24)]. For the case of THz emitters fabricated on RDSOS, the relatively low value of dc carrier mobility μ_{dc} yields the relatively high value $F_{\mathrm{sat}}^{\mathrm{bb}} = 0.25\ \mathrm{mJ/cm^2}$.[6] For III–V semiconductors such as GaAs and InP, however, much higher carrier mobilities may be achieved in materials with comparably short photocurrent relaxation times τ_d. For example, from Eq. (24) we estimate a broadband saturation fluence of $F_{\mathrm{sat}}^{\mathrm{bb}} = 5.2\ \mu\mathrm{J/cm^2}$ for GaAs-based photoconductors.[13] This implies that one could obtain enhancements comparable with those calculated for RDSOS-based emitters at much lower narrow-band excitation fluences.

Thus the theory of saturation developed in this paper

indicates that to achieve a large enhancement in spectral brightness for narrow-band THz emission we must choose a photoconductive medium with a short photocurrent relaxation time. The preceding paragraph further suggests that a photoconductor with a low broadband saturation fluence is desirable to avoid entering a regime of high fluence where effects neglected in the theory may dominate. Materials such as low-temperature-grown GaAs appear to be attractive choices to fulfill both criteria.

Before leaving this discussion we would like to consider explicitly how our analysis of saturation in narrow-band emitters might be applied to different experimental conditions. In particular, we wish to examine the two limiting cases, one in which the area of the THz emitter is restricted and another in which the available laser fluence is restricted. Inasmuch as the conversion of laser radiation to THz radiation is an inherently nonlinear process, the optical-to-THz conversion efficiency scales with the absorbed optical intensity up to the point of saturation. Therefore, to achieve optimal efficiency, we always wish to arrange conditions so as reach the full saturation fluence. This implies that, if one is restricted to a given available area for a photoconducting mixer, one should increase the laser pulse energy to attain the saturation fluence. Conversely, if one is restricted to a given laser fluence, one should focus the pump laser radiation sufficiently tightly so that it will reach the saturation fluence.

As shown above, the saturation fluence of the emitter is increased by a factor of α for chirped-pulse excitation compared with ultrashort-pulse excitation. For the case of an emitter of limited area but arbitrary laser pulse energy, we would raise the laser pulse energy for narrow-band excitation by a factor of α relative to that for broadband excitation. It follows that we obtain an enhancement in the spectral irradiance by a factor of the order of α^2 and that the efficiency of the THz generation process within the desired spectral bandwidth will increase by a factor of α (Fig. 1). For excitation with limited laser energy, we would focus the narrow-band laser beam tightly enough to reach the higher narrow-band saturation fluence. In this event, according to Eq. (35) above, the spectral irradiance of the narrow-band output will be higher than that for broadband output by a factor of α^2. However, because the effective emitter area A for the broadband THz output will be reduced by a factor α, the power spectral density $[P(\Omega) = AS(\Omega)]$ of the narrow-band output will be higher only by a factor of α. The increase in the efficiency of the THz generation process [Eq. (36)] in the desired spectral width will also increase by a factor α, as in the previous case.

4. EXPERIMENTAL RESULTS

To examine the possibility of such enhanced performance experimentally, we used a self-mode-locked Ti:sapphire laser as a source of ~11-nm (FWHM) bandwidth pulses of a wavelength of 800 nm and a duration of 110 fs (FWHM). This laser operated at a repetition rate of 76 MHz and provided an average power of 0.6 W. The experimental setup for producing and mixing stretched optical pulses is similar to that employed previously.[16,18] The dispersive delay line consisted of a pair of parallel holographic diffraction gratings (1800 lines/mm), which we used in a double-pass configuration to obtain chirped pulses of ~100 ps FWHM. A Michelson interferometer served to split the stretched optical pulse into two halves and mix the two parts after introducing a variable time delay τ between them.[18] The THz emitter and detector were identical 50 μm-long dipole emitters fabricated on RDSOS. The dipole structure had a 5-μm-wide active photoconducting gap and loaded a coplanar transmission line structure composed of 2-cm-long, 10-μm-wide, 1-μm-thick Al electrodes. The Si epilayer was 0.6 μm in thickness and was ion implanted to reduce the carrier lifetime. The implantation process involved a 10^{15}/cm^2 dose of O^+ ions at 100 keV followed by a 10^{15}/cm^2 dose of O^+ ions at 200 keV at beam current densities below 0.1 μA/cm^2 to avoid annealing. The carrier recombination lifetime of the Si in this case has been measured by time-resolved reflectivity to be ~0.6 ps.[24] Although the theory in this paper has been formulated in terms of large-aperture photoconductive emitters, for the experiment we employed a dipole structure. This choice was dictated by the limited pulse energy available from the Ti:sapphire laser source, which required tight focusing of the pump beam to reach a regime of saturated response.

We generated THz radiation by exciting one of the photoconducting dipoles biased at 5 V with either broadband or narrow-band optical excitation pulses. We recorded the resulting THz waveforms by measuring the average current in the detecting dipole, which was gated by a 10-mW probe beam. Both the pump and the probe beams were focused through identical 10× microscope objectives to yield spot sizes of ~10 μm. Off-axis paraboloidal mirrors and hyperhemispherical lenses of high-resistivity Si were used to transport the emitted THz radiation from the generator to the detector.[2] The THz radiation was modulated at ~1 kHz by a mechanical chopper in the path of the pump laser beam. This scheme permitted the average photocurrent in the detector to be measured by a lock-in amplifier. We confirmed that thermal effects owing to the high average intensity of the pump (as high as 300 kW/cm^2) did not influence the saturation behavior of the dipole antennas in either the broadband or the narrow-band case. We did this by comparing the behavior of the THz emission for two different duty cycles (0.5 and 0.167) for the pump beam. The THz field amplitudes were within ±10% of each other for the two duty cycles at all relevant pump pulse energies.

Figure 5 displays the measured variation of spectral irradiance $S(\Omega)$ of the THz radiation as a function of the absorbed laser fluence, i.e., the saturation characteristics of the emitter. The fact that the experimental pump beam profile varies spatially requires the determination of an effective fluence incident upon the dipole emitter. We made this determination by weighting different portions of the pump beam by a function that reflects the contribution of each portion of the beam to the THz output. Because the THz spectral irradiance scales quadratically with the laser intensity (neglecting saturation), the effective pump fluence incident upon the emitter is given by

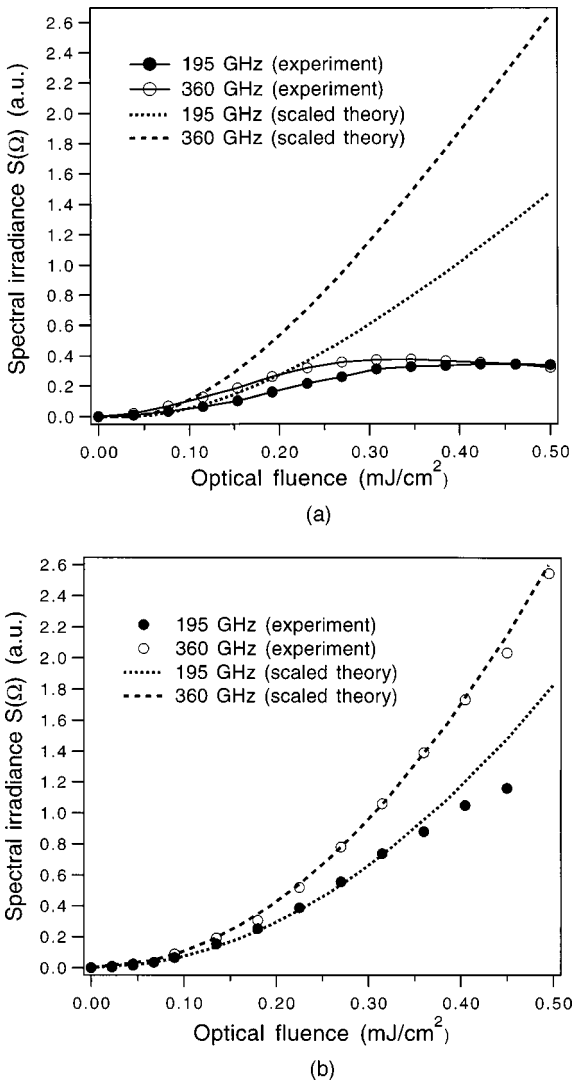

Fig. 5. Experimental results of the variation of the THz spectral irradiance $S(\Omega)$ with absorbed optical fluence for (a) broadband (~110-fs FWHM pulses) and (b) narrow-band (obtained by mixing of two 100-ps FWHM chirped pulses with a variable delay) excitation at 800 nm of RDSOS dipole emitters. Dashed curves, values of $S(\Omega)$ calculated numerically from the model for saturation described in text. The scale of the numerically calculated curves has been adjusted to match the experimental results at low fluence.

$$F_{\mathrm{inc}} = \frac{\int_{-\infty}^{\infty}\int_{-\infty}^{\infty} \mathrm{d}x\,\mathrm{d}y[F(x,y)]^2 F(x,y)}{\int_{-\infty}^{\infty}\int_{-\infty}^{\infty} \mathrm{d}x\,\mathrm{d}y[F(x,y)]^2}, \qquad (39)$$

where $F(x, y)$ is spatial distribution of the laser fluence. For a Gaussian beam profile given by $F(x, y) = F_0 \exp[-(x^2 + y^2)/\rho^2]$, Eq. (39) yields an effective fluence of

$$F_{\mathrm{inc}} = (2/3)F_0 = (2/3)(E_{\mathrm{inc}}/\pi\rho^2), \qquad (40)$$

where E_{inc} is the incident pump pulse energy. We experimentally measured ρ for the pump beam to be 6 μm. We determined the fraction of incident fluence F_{inc} absorbed [β in Eq. (3)] by measuring the fraction reflected from and the fraction transmitted through the detector. We found a value of $\beta \sim 0.29$ at normal incidence. The results for the variation of $S(\Omega)$ with absorbed laser fluence (βF_{inc}) are shown in Fig. 5(a) for broadband excitation and in Fig. 5(b) for narrow-band excitation. The values of $S(\Omega)$ were obtained from the numerical Fourier transforms of the time-domain data. In the figure we also display the corresponding values of $S(\Omega)$ calculated numerically from the saturation model in Subsection 3.B for the relevant beat frequencies.

5. DISCUSSION OF RESULTS

The experimental data for broadband excitation presented in Fig. 5(a) show clear evidence of saturation of the THz spectral irradiance. On the other hand, for the case of narrow-band excitation in Fig. 5(b) there is no noticeable deviation from the ideal behavior at comparable fluences. In our experiments we were unable to achieve saturation of the THz spectral brightness for the case of narrow-band optical excitation, even with the maximum pump fluence available from our laser source. We now address experimental data obtained in each of the two excitation schemes separately and examine implications for trends in the enhancement of saturation fluence and THz spectral brightness. In the discussion below, we use the earlier definition of saturation fluence for both broadband and narrow-band excitation, i.e., the fluence at which the value of $S(\Omega)$ is half of its ideal value in the absence of saturation ($\theta = 0.5$).

Figure 5(a) for spectral irradiance $S(\Omega)$ under broadband excitation shows strong saturation effects over the available range of pump fluences. Over the same range of fluences, however, there is weaker deviation from ideality in the values of $S(\Omega)$ calculated from our model for saturation of large-aperture THz emitters. The scale for $S(\Omega)$ of the numerically calculated curves (dashed curves) has been adjusted to fit the experimental data at low fluences. From a fit to these experimental data we estimate the broadband saturation fluence $F_{\mathrm{sat}}^{\mathrm{bb}}$ for our dipole emitters (for $\theta = 0.5$) to be 0.14 and 0.17 mJ/cm^2 at the two experimental values of the THz frequency Ω. These values are significantly lower than the corresponding values of 0.51 and 0.65 mJ/cm^2 obtained for $F_{\mathrm{sat}}^{\mathrm{bb}}$ from the numerical calculations based on our model for saturation of the THz emission from large-aperture RDSOS emitters. This discrepancy suggests that our model of saturation for large-aperture emitters may be inadequate to account for saturation of the micrometer-sized dipole emitters that we have used in our experiments. Pedersen *et al.*[25] showed that saturation from screening of the bias field by space-charge effects, i.e., the physical separation of the photogenerated carriers under the applied bias field, is expected to be significant for emitters with such small illuminated areas, whereas the treatment above has neglected this effect. An electrostatic model for the bias field dynamics that is due to such space-charge effects has been developed by Jacobsen *et al.*[26] To obtain a more comprehensive picture of the saturation of the THz field in our experiment, we would have to include these effects in our calculation of the screening of the bias

field,[21,23] which could be expected to lead to saturation effects at lower absorbed fluences.

For the case of narrow-band excitation, the data in Fig. 5(b) show no appreciable saturation effects over the range of absorbed fluence available in our experiments. For narrow-band excitation of a RDSOS photoconductor ($\tau_d = 0.6$ ps) with a 100-ps-long chirped pulse, our model predicts a saturation fluence of $F_{\mathrm{sat}}^{\mathrm{nb}} = 26\ \mathrm{mJ/cm^2}$. However, if we included the effects of space-charge screening discussed above, we would expect $F_{\mathrm{sat}}^{\mathrm{nb}}$ to be considerably lower. A key parameter that influences the enhancement in saturation fluences in our model is the decay time of the dominant saturation mechanism. Jacobsen *et al.*[26] observed in their experiments on RDSOS dipole emitters that space-charge screening of the bias field decayed on the time scale of recombination lifetime of photogenerated electrons. Inasmuch as we used pump fluences similar to those used in their experiments, we would expect the decay time of saturation effects in our dipole emitters to be given approximately by $\tau_d \cong 0.6$ ps, the carrier recombination lifetime in RDSOS.

The general arguments developed above for the enhancement in saturation fluence obtained by use of narrow-band excitation compared with broadband excitation are applicable to any saturation mechanism, provided that its recovery time remains short compared with the duration of the narrow-band optical pulse. Therefore, although the value of the saturation fluence would be modified by the inclusion of space-charge screening effects, we expect enhancement α in saturation fluence to be given approximately by $\alpha = (T_{\mathrm{eff}}/\tau_d)$. If we use the experimental values of $F_{\mathrm{sat}}^{\mathrm{bb}}$ mentioned above, this corresponds to a narrow-band saturation fluence $F_{\mathrm{sat}}^{\mathrm{nb}} \cong 4\ \mathrm{mJ/cm^2}$ for excitation with 100-ps-long chirped pulses used in our experiment. This saturation fluence is significantly greater than the maximum pump fluence available from our laser source. However, we can derive a lower bound on the experimental value of $F_{\mathrm{sat}}^{\mathrm{nb}}$ by scaling the theoretical variation of $S(\Omega)$ with optical fluence to fit our experimental data. We estimate this bound to be $\geqslant 1.5\ \mathrm{mJ/cm^2}$, which implies that we have achieved an enhancement $\alpha \geqslant 10$ in the saturation fluence.

Our experimental data confirm a significant enhancement in the saturation fluence for narrow-band excitation. Such an enhancement α in the saturation fluence should lead under optimal conditions to an enhancement in THz spectral irradiance $S(\Omega)$ of the order of $\alpha^2/10$, a factor of >10 in our case. We have not, however, attempted to estimate the enhancement in $S(\Omega)$ achieved by using narrow-band excitation in our experiment. This reflects limitations involved in the direct comparison of values of $S(\Omega)$ in the narrow-band and broadband cases. Such a comparison could be strongly influenced by the presence of an imperfect spatial overlap between the two chirped pulses, which might cause spatial steering of the narrow-band THz radiation.[18] Also, any nonidealities in our dispersion line would produce cubic and higher-order phase distortions in the chirped excitation pulses and cause a decrease in the narrow-band spectral brightness relative to the ideal case of perfectly linear chirp.[18] We expect, nonetheless, that the equivalence of the narrow-band and the broadband spectral irradiance will be observed in the unsaturated regime for a suitable experimental geometry. In this instance we would also expect to observe significant enhancements in $S(\Omega)$ at high fluences as predicted by our model.

6. CONCLUSIONS

We have demonstrated the enhancement of the saturation fluence of photoconducting emitters by using narrow-band excitation obtained by mixing two linearly chirped optical excitation pulses. The physical origin of this enhancement is the reduction of saturation in the THz output by screening of the bias field by the photocurrent, which we achieved by spreading out the excitation over several photocurrent decay time intervals. The chirped-pulse mixing scheme provides a method for using longer optical excitation pulses while retaining access to the full range of THz frequencies produced with short-pulse excitation. From the existing model for the saturation behavior of large-aperture emitters, we have shown that the saturation fluence for chirped-pulse mixing is higher than for broadband excitation by a factor that is proportional to the ratio of the duration of the chirped pulses to the photocurrent relaxation time and is essentially independent of the THz beat frequency. Within the context of an approximate analytic theory, we have obtained an explicit expression for the increase in the saturation fluence and the consequent enhancement in spectral irradiance for narrow-band excitation. For the case of mixing chirped Gaussian pulses with a duration T (FWHM), we expect an enhancement in the saturation fluence of $\alpha = 0.393\ (T/\tau_d)$, where τ_d is the photocurrent relaxation time. Such improvements in the saturation fluence of emitters excited in the chirped-pulse mixing scheme should permit the efficient utilization of fluences of the order of $\mathrm{mJ/cm^2}$ currently available from amplified femtosecond laser systems. With respect to corresponding improvement in the THz output of photoconductive emitters, an increase in saturation fluence by a factor of α implies an enhancement in spectral irradiance for narrow-band excitation that scales as α^2.

Our experimental results for photoconductive dipole emitters fabricated upon radiation-damaged silicon-on-sapphire samples have confirmed the predicted increase in saturation fluence for chirped-pulse excitation, with an observed enhancement in saturation fluence that exceeds a factor of 10. A more comprehensive verification of the results of our calculations would be expected for measurements of saturation in large-aperture photoconductors excited by the high-energy pulses that are available with an amplified femtosecond laser system. Another useful direction that could be explored involves employing photoconductors with different carrier lifetimes. In this context, one could examine the saturation characteristics of radiation-damaged GaAs emitters with different ion-implantation doses.[27] Because they combine the desirable properties of high transient mobility, low carrier lifetime, and higher electrical breakdown field,[28] GaAs-based photoconductors appear to present a material system superior to RDSOS in terms of exploiting fully the enhancements in THz brightness afforded by chirped-pulse beating. Liu *et al.* recently demonstrated such an en-

hancement in narrow-band THz radiation generated with dipole antennas made on low-temperature-grown GaAs (Ref. 17) but did not explore the full potential of these devices for intense THz generation.

ACKNOWLEDGMENTS

We would like to thank Jim Misewich of IBM, Yorktown Heights, for fabrication of the RDSOS dipole antennas used in our experiments and David Auston, Jie Shan, and Ajay Nahata for many helpful discussions. This research was supported by the National Science Foundation under the grant CHE-96-12294 and by the U.S. Air Force Office of Scientific Research under grant F49620-98-1-0137.

REFERENCES

1. P. R. Smith, D. H. Auston, and M. C. Nuss, "Subpicosecond photoconducting dipole antennas," IEEE J. Quantum Electron. **24**, 255 (1988).
2. M. Van Exter and D. Grischkowsky, "Characterization of an optoelectronic terahertz beam system," IEEE Trans. Microwave Theory Tech. **38**, 1684 (1990).
3. B. B. Hu, X.-C. Zhang, and D. H. Auston, "Free space radiation from electro-optic crystals," Appl. Phys. Lett. **56**, 506 (1990).
4. B. B. Hu, J. T. Darrow, X.-C. Zhang, D. H. Auston, and P. R. Smith, "Optically steerable photoconducting antennas," Appl. Phys. Lett. **56**, 886 (1990).
5. Q. Wu and X.-C. Zhang, "Free-space electro-optic sampling of THz beams," Appl. Phys. Lett. **67**, 3523 (1995); A. Nahata, D. H. Auston, T. F. Heinz, and C. Wu, "Coherent detection of freely propagating terahertz radiation by electro-optic sampling in a poled polymer," Appl. Phys. Lett. **68**, 150 (1996); P. Uhd Jepsen, C. Winnewisser, M. Schall, V. Schyja, S. R. Keiding, and H. Helm, "Detection of THz pulses by phase retardation in lithium tantalate," Phys. Rev. E **53**, R3052 (1996).
6. D. Grischkowsky, "Nonlinear generation of subpicosecond pulses of THz electromagnetic radiation by optoelectronics—applications to time-domain spectroscopy," in *Frontiers in Nonlinear Optics*, H. Walther, N. Koroteev, and M. O. Scully, eds. (Institute of Physics, Philadelphia, Pa., 1993), pp. 196–227.
7. B. B. Hu and M. C. Nuss, "Imaging with terahertz waves," Opt. Lett. **20**, 1716 (1995); Q. Wu, T. D. Hewitt, and X.-C. Zhang, "Two-dimensional electro-optic imaging of THz beams," Appl. Phys. Lett. **69**, 1026 (1996).
8. R. A. Cheville and D. R. Grischkowsky, "Time-domain terahertz impulse ranging studies," Appl. Phys. Lett. **67**, 1960 (1995).
9. B. I. Greene, P. N. Saeta, D. R. Dykaar, S. Schmitt-Rink, and S. L. Chuang, "Far-infrared light generation at semiconductor surfaces and its spectroscopic applications," IEEE J. Quantum Electron. **28**, 2302 (1992).
10. R. R. Jones, N. E. Tielking, D. You, C. Raman, and P. H. Bucksbaum, "Ionization of oriented Rydberg states by subpicosecond half-cycle electromagnetic pulses," Phys. Rev. A **51**, R2687 (1995).
11. D. You, R. R. Jones, P. H. Bucksbaum, and D. R. Dykaar, "Generation of high-power sub-single-cycle 500-fs electromagnetic pulses," Opt. Lett. **18**, 290 (1993); E. Budiarto, J. Margolies, S. Jeong, J. Son, and J. Bokor, "High-intensity terahertz pulses at 1-kHz repetition rate," IEEE J. Quantum Electron. **32**, 1839 (1996).
12. J. T. Darrow, X.-C. Zhang, D. H. Auston, and J. D. Morse, "Saturation properties of large-aperture photoconducting antennas," IEEE J. Quantum Electron. **28**, 1607 (1992).
13. P. K. Benicewicz, J. P. Roberts, and A. J. Taylor, "Scaling of terahertz radiation from large-aperture biased photoconductors," J. Opt. Soc. Am. B **11**, 2533 (1994).
14. A. Mayer and F. Keilmann, "Far-infrared nonlinear optics: I & II," Phys. Rev. B **33**, 6954 (1986).
15. A. S. Weling and T. F. Heinz, "Photoconducting terahertz emitters with enhanced spectral brightness," in *Conference on Lasers and Electro-Optics*, Vol. 11 of OSA Technical Digest Series (Optical Society of America, Washington, D.C., 1997), paper CTuC7.
16. A. S. Weling, B. B. Hu, N. M. Froberg, and D. H. Auston, "Generation of tunable narrowband THz radiation from large aperture photoconducting antennas," Appl. Phys. Lett. **64**, 137 (1994).
17. Y. Liu, S.-G. Paek, and A. M. Weiner, "Enhancement of narrow-band terahertz radiation from photoconducting antennas by optical pulse shaping," Opt. Lett. **21**, 1762 (1996); Y. Liu, S.-G. Paek, and A. M. Weiner, "Terahertz waveform synthesis via optical pulse shaping," IEEE J. Sel. Top. Quantum Electron. **2**, 709 (1996).
18. A. S. Weling and D. H. Auston, "Novel sources and detectors for coherent tunable narrowband terahertz radiation in free space," J. Opt. Soc. Am. B **13**, 2783 (1996).
19. See, for example, J. W. Goodman, *Statistical Optics* (Wiley, New York, 1985), Chap. 3.
20. W. Sha, J.-K. Rhee, T. B. Norris, and W. J. Schaff, "Transient carrier and field dynamics in quantum-well parallel transport: from the ballistic to the quasi-equilibrium regime," IEEE J. Quantum Electron. **28**, 2445 (1992); T. Dekorsy, T. Pfeiffer, W. Kutt, and H. Kurz, "Subpicosecond carrier transport in GaAs surface-space-charge fields," Phys. Rev. B **47**, 3842 (1993).
21. G. Rodriguez and A. J. Taylor, "Screening of the bias field in terahertz radiation from photoconductors," Opt. Lett. **21**, 1046 (1996).
22. A. J. Taylor, P. K. Benicewicz, and S. M. Roberts, "Modeling of femtosecond electromagnetic pulses from large-aperture photoconductors," Opt. Lett. **18**, 1340 (1993).
23. A. J. Taylor, G. Rodrigues, and D. Some, "Ultrafast field dynamics in large-aperture photoconductors," Opt. Lett. **22**, 715 (1997).
24. F. Doany, D. Grischkowsky, and C.-C. Chi, "Carrier lifetime versus ion-implantation dose in silicon-on-sapphire," Appl. Phys. Lett. **50**, 460 (1987).
25. J. E. Pedersen, V. G. Lyssenko, J. M. Hvam, P. Uhd Jepsen, S. R. Keiding, C. B. Sorensen, and P. E. Lindelof, "Ultrafast local field dynamics in photoconductive THz antennas," Appl. Phys. Lett. **62**, 1265 (1993).
26. R. H. Jacobsen, K. Birkelund, T. Holst, P. Uhd Jepsen, and S. R. Keiding, "Interpretation of photocurrent correlation measurements used for ultrafast photoconductive switch characterization," J. Appl. Phys. **79**, 2649 (1996).
27. A. Krotkus, S. Marcinkevicius, J. Jasinski, M. Kaminska, H. H. Tan, and C. Jagadish, "Picosecond carrier lifetime in GaAs implanted with high doses of As ions: an alternative material to low-temperature GaAs for optoelectronic applications," Appl. Phys. Lett. **66**, 3304 (1995); M. Lambsdorff, J. Kuhl, J. Rosenzweig, A. Axmann, and J. Schneider, "Subpicosecond carrier lifetimes in radiation-damaged GaAs," Appl. Phys. Lett. **58**, 1881 (1991).
28. E. R. Brown, K. A. Macintosh, K. B. Nichols, and C. L. Dennis, "Photomixing up to 3.8 THz in low-temperature-grown GaAs," Appl. Phys. Lett. **66**, 285 (1995).